MODELLING OF SUBMERGED
CABLE DYNAMICS

James W. Kamman

and

Ronald L. Huston

Department of Mechanical
and Industrial Engineering
Location 72
University of Cincinnati
Cincinnati, Ohio 45221

DTIC
ELECTE
SEP 1 6 1983
E

83 09 14 084

REPORT DOCUMENTATION PAGE		READ INSTRUCTIONS BEFORE COMPLETING FORM
1. REPORT NUMBER ONR-UC-MIE-070183-16	2. GOVT ACCESSION NO.	3. RECIPIENT'S CATALOG NUMBER
4. TITLE (and Subtitle) Modelling of Submerged Cable Dynamics		5. TYPE OF REPORT & PERIOD COVERED Technical 7/1/80 - 7/1/83
		6. PERFORMING ORG. REPORT NUMBER
7. AUTHOR(s) James W. Kamman and Ronald L. Huston		8. CONTRACT OR GRANT NUMBER(s) N00014-76C-0139
9. PERFORMING ORGANIZATION NAME AND ADDRESS University of Cincinnati Cincinnati, OH 45221		10. PROGRAM ELEMENT, PROJECT, TASK AREA & WORK UNIT NUMBERS 122303
11. CONTROLLING OFFICE NAME AND ADDRESS ONR Resident Research Representative Ohio State University, 1314 Kenner Rd. Columbus, OH		12. REPORT DATE 7/1/83
		13. NUMBER OF PAGES 35
14. MONITORING AGENCY NAME & ADDRESS(If different from Controlling Office) Office of Naval Research Structural Mechanics Department of the Navy Arlington, VA 22217		15. SECURITY CLASS. (of this report) Unclassified
		15a. DECLASSIFICATION/DOWNGRADING SCHEDULE

16. DISTRIBUTION STATEMENT (of this Report)

Distribution of this report is unlimited.

17. DISTRIBUTION STATEMENT (of the abstract entered in Block 20, If different from Report)

18. SUPPLEMENTARY NOTES

19. KEY WORDS (Continue on reverse side if necessary and identify by block number)

Cable Dynamics, Mooring, Anchors, Bouys, Finite Segment Modelling

20. ABSTRACT (Continue on reverse side if necessary and identify by block number)

Results from a series of simulated submerged cable maneuvers are presented. The simulations are obtained using a three-dimensional, finite-segment model of the cable. The model, called UCIN-CABLE, consists of a series of pin connected rigid rods. Fluid drag, inertia, and buoyancy forces are included.

Two types of simulation are presented: buoy release and anchor drop. The results compare favorably with experimental data and with data obtained from finite-element modelling.

ABSTRACT

Results from a series of simulated submerged cable maneuvers are presented. The simulations are obtained using a three-dimensional, finite-segment model of the cable. The model, called UCIN-CABLE, consists of a series of ball-and-socket connected rigid rods. Fluid drag, inertia and buoyancy forces are included.

Two types of simulation are presented: buoy release and anchor drop. The results compare favorably with experimental data and with data obtained from finite-element modelling.

Accession For	
NTIS GRA&I	☒
DTIC TAB	☐
Unannounced	☐
Justification	

By
Distribution/

Availability Codes	
Dist	Avail and/or Special
A	

NOTATION

a Cross section area of L_j.

a,b,c Coefficients defined by Equations (26),(27) and (28).

$\underset{\sim}{a}_{GN}$ Component of fluid acceleration normal to L_j at G_j. [See Equation (24).]

$\underset{\sim}{a}_N$ Normal component of fluid acceleration relative to L_j at P.

$\underset{\sim}{a}_{W/G}$ Acceleration of the fluid relative to G_j.

$a_{\ell p}$ Mass matrix. [See Equations (1) and (2).] $(\ell,p=1,\ldots,n)$

A,B,C Coefficients defined by Equations (5),(6) and (7).

$\underset{\sim}{b}_N$ Buoyancy force on L_j at P, per unit length.

$\underset{\sim}{B}_N$ Equivalent buoyancy force on L_j at G_j. [See Equation (19).]

C_M, C_N, C_T Coefficients defined by Equations (8), (9), and (10).

d Diameter of L_j.

e_{mnk} Permutation symbol.

$\underset{\sim}{f}$ Applied force on L_j at P. [See Equation (4).]

f_ℓ Defined by Equation (3). $(\ell=1,\ldots,n)$

$\underset{\sim}{F}_j$ Equivalent applied force on L_j at G_j. [See Equation (15).]

F_{jk} $\underset{\sim}{n}_k$ components of F_j. $(j=1,\ldots,N;\ k=1,2,3)$

$\underset{\sim}{F}_M$ Equivalent added mass force on L_j at G_j. [See Equation (17).]

$\underset{\sim}{F}_N$ Equivalent normal drag force on L_j at G_j. [See Equation (18).]

$\underset{\sim}{F}_T$ Equivalent tangential drag force on L_j at G_j. [See Equation (19).]

F_ℓ Generalized active forces. $(\ell=1,\ldots,n)$

g Gravity constant.

G_j Mass center of L_j. $(j=1,\ldots,N)$

I_{jkh} $\underset{\sim}{n}_k$ components of the inertia dyadic of L_j with respect to G_j. $(j=1,\ldots,N;\ k,h=1,2,3)$

$\underset{\sim}{k}$ Vertical (up) unit vector.

L Length of L_j.

L_j Typical cable segment. $(j=1,\ldots,N)$

m_j Mass of segment L_j.

n Number of degrees of freedom.

$\underset{\sim}{n}$ Unit vector parallel to L_j.

$\underset{\sim}{n}_k$ Unit vectors fixed in R. $(k=1,2,3)$

N Number of cable segments.

P A typical point on L_j.

R	An inertial reference frame.
R_{eN}, R_{eT}	Reynolds numbers defined by Equations (11) and (12).
$\underset{\sim}{T}_j$	Equivalent applied torque on L_j. [See Equation (16).]
T_{jk}	$\underset{\sim}{n}_k$ components of $\underset{\sim}{T}_j$. $\qquad (j=1,\ldots,N;\ k=1,2,3)$
$\underset{\sim}{T}_M$	Equivalent added mass torque on L_j. [See Equation (22).]
T_N	Equivalent normal drag torque on L_j. [See Equation (23).]
v_{jpk}	$\underset{\sim}{n}_k$ components of the partial velocity of G_j. $\qquad (j=1,\ldots,N;\ p=1,\ldots,n;\ k=1,2,3)$
$\underset{\sim}{v}_{GN}$	Components of fluid velocity normal to L_j at G_j. [See Equation (25).]
$\underset{\sim}{V}_N$	Normal component of fluid velocity relative to L_j at P.
$\underset{\sim}{V}_T$	Tangential component of fluid velocity relative to L_j at P.
$\underset{\sim}{V}_{W/G}$	Velocity of the fluid relative to G_j.
$\underset{\sim}{w}$	Weight of L_j per unit length.
$\underset{\sim}{W}$	Weight of L_j. [See Equation (20).]
X_p	Orientation angles. $\qquad (p=1,\ldots,n)$
μ	Viscoscity of the fluid.
ρ	Fluid mass density.
ρ_c	Cable mass per unit length.
ω_{jpk}	$\underset{\sim}{n}_k$ components of the partial angular velocity of L_j. $\qquad (j=1,\ldots,N;\ p=1,\ldots,n;\ k=1,2,3)$

INTRODUCTION

In a series of recent papers [1,2,3]*, we presented a method for modelling cable dynamics. The method is based upon previously developed general procedures for finite segment modelling of multibody systems [4,5]. In this report we present results obtained by applying the method in a series of submerged cable configurations. The results are compared with experimental data reported by Palo at the Navy's Civil Engineering Laboratory [6], and with numerical data obtained from SEADYN [7]--a finite element cable computer code.

A brief review of the method itself is presented in the first section of the report.

---

*Numbers in brackets refer to References at the end of the report.

I. FINITE SEGMENT MODELLING

We model a cable by a series of ball-and-socket connected rigid links, or segments, as depicted in Figure 1. The dimensions and physical parameters of the segments are arbitrary. Also, we let the segments be subjected to general force fields. This allows us to simulate an arbitrary fluid environment, as well as gravity and buoyancy forces. Finally, cable stiffness or elasticity, if it is significant, can be modelled by springs and dampers between the segments.

We describe the orientation and configuration of the system using the relative angles between the segments. We assume that in a specific maneuver that one end of the cable may be attached to a towed body and that the motion of the other end is specified (for example, it may be fixed). We assume that the initial configuration of the system is known. The objective of the analysis is then to define the subsequent configuration of the system.
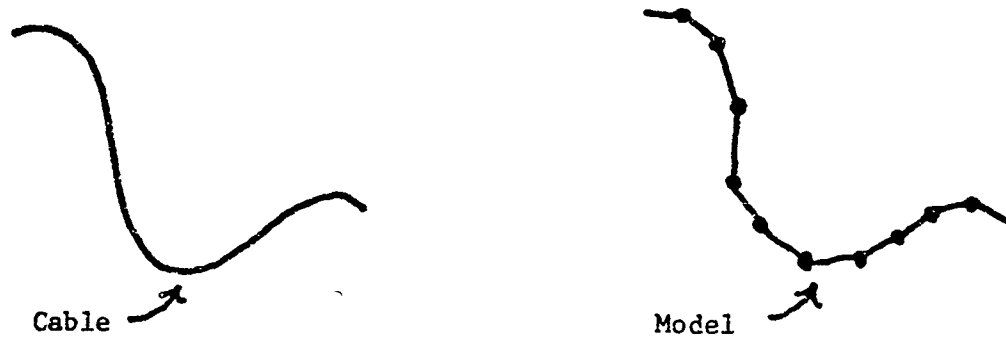
Cable   Model

Figure 1. A Finite Segment Model of a Cable.

Using procedures developed for finite segment modelling of multi-body systems [4,5], we can obtain explicit governing dynamical equations of motion for the cable model. What is more, we can obtain these equations in a form suitable for conversion into algorithms for numerical integration. Specifically, the equations may be written in the form:

$$a_{\ell p} \ddot{X}_p = f_\ell \qquad (\ell, p = 1, \ldots, n) \qquad (1)$$

where the $X_p (p=1,\ldots,n)$ represent the relative orientation angles of the cable segments, where n is the number of degrees of freedom. (Regarding notation, there is a sum for repeated indices over the range of the index.) $a_{\ell p}$ and f_ℓ are given by the expressions:

$$a_{\ell p} = m_j v_{jpk} v_{j\ell k} + I_{jkh} \omega_{jph} \omega_{j\ell k} \qquad (2)$$

and

$$f_\ell = F_\ell - (m_j v_{j\ell k} \dot{v}_{jqk} \dot{X}_q + I_{jkh} \omega_{j\ell h} \dot{\omega}_{jqk} \dot{X}_q$$
$$+ e_{mnk} \omega_{jqn} \omega_{jsr} \omega_{j\ell k} I_{jmr} \dot{X}_q \dot{X}_s) \qquad (3)$$

where $m_j (j=1,\ldots,N)$ is the mass of the jth cable segment L_j, N is the number of cable segments; $I_{jkh} (k,h=1,2,3)$ are the components of I_j, the inertia dyadic of L_j with respect to its mass center G_j, referred to unit vectors n_k fixed in an inertial reference frame R; ω_{jpk} and v_{jpk} $(j=1,\ldots,N; p=1,\ldots,n; k=1,2,3)$ are the n_k components of the partial angular velocities and partial velocities of L_j and G_j [8]; $F_\ell (\ell=1,\ldots,n)$ are the generalized active forces [8] developed from the forces applied to L_j; and e_{mnk} is the permutation symbol [9].

Equations (1) form a set of n simultaneous nonlinear ordinary differential equations determining the orientation angles X_p. Since the coefficients $a_{\ell p}$ and f_ℓ are functions of the arrays $v_{j\ell k}$ and $\omega_{j\ell k}$ and their derivatives, the system of governing equations can automatically be generated once the $v_{j\ell k}$ and $\omega_{j\ell k}$ arrays and their derivatives are determined. Simple algorithms for computing $v_{j\ell k}$ and $\omega_{j\ell k}$ and their derivatives have been developed. They are recorded in References [4] and [5].

II. FLUID AND GRAVITY FORCE MODELLING

The applied forces contributing to the generalized active forces F_ℓ consist of fluid and gravity forces. The fluid forces may be represented as: 1) Normal drag forces; 2) Tangential drag forces; 3) Added mass forces; and 4) Buoyancy forces. Reference [2] contains a detailed analysis of each of these forces. Specifically, it is shown in [2] that the applied force at a typical point P (See Figure 2.) of a segment L_j may be written as:

$$\underline{f} = A\underline{a}_N + B|\underline{V}_N|\underline{V}_N + C|\underline{V}_T|\underline{V}_T + \underline{w} + \underline{b}_N \tag{4}$$

where $\underline{V}_N$ is the normal component of the fluid velocity relative to the cable segment at P, $\underline{a}_N$ is the normal component of the fluid acceleration relative to the cable segment at P, $\underline{V}_T$ is the tangential component of the fluid velocity relative to the cable segment at P, $\underline{w}$ is the segment weight per unit length, and $\underline{b}_N$ is the buoyancy force per unit length.
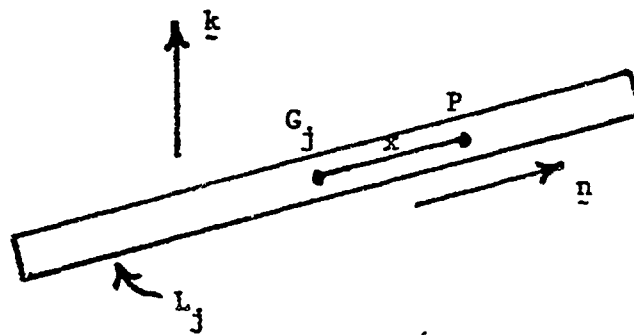
Figure 2. A Typical Cable Segment L_j.

The coefficients A, B, and C are:

$$A = C_M \rho (\pi/4) d^2 \tag{5}$$

$$B = C_N \rho (d/2) \tag{6}$$

$$C = C_T \rho (d/2) \tag{7}$$

where ρ is the fluid mass density and d is the diameter of L_j. C_M, C_N, and C_T are coefficients dependent upon the Reynolds number of the fluid flow relative to the cable segment. They are usually determined experimentally and reported results may vary slightly. Webster [7] records them as

$$C_M = 1.0 \tag{8}$$

$$C_N = \begin{cases} 0.0 \text{ for } R_{eN} \leq 0.1 \\ 0.45 + 5.93/(R_{eN})^{0.33} \text{ for } 0.1 < R_{eN} \leq 400.00 \\ .27 \text{ for } 400 < R_{eN} \leq 10^5 \\ 0.3 \text{ for } R_{eN} > 10^5 \end{cases} \tag{9}$$

and

$$C_T = \begin{cases} 1.88/(R_{eT})^{0.74} \text{ for } 0.1 < R_{eT} \leq 100.55 \\ 0.062 \text{ for } R_{eT} > 100.55 \end{cases} \tag{10}$$

where the Reynolds numbers R_{eN} and R_{eT} are defined as:

$$R_{eN} = \rho d |V_N|/\mu \tag{11}$$

and

$$R_{eT} = \rho d |V_T|/\mu \tag{12}$$

where μ is the viscoscity of the fluid.

The weight force w may be expressed as:

$$w = -\rho_c g k \tag{13}$$

where ρ_c is the cable mass per unit length, g is the gravity constant, and $\underline{k}$ is a vertical (up) unit vector.

The buoyancy force at P may be expressed as [2]

$$\underline{b}_N = \rho g a \, \underline{n} x(\underline{k} \times \underline{n}) \tag{14}$$

where a is the cross section area of L_j and $\underline{n}$ is a unit vector parallel to L_j. (See Figure 2.) (Note that since the cable segment is a model of a portion of a continuous cable, the ends of the segment are not exposed to the fluid. That is, the segment ends are "shielded" from the fluid by the adjoining cable segments. This results in $\underline{b}_N$ being normal to L_j.)

If the set of applied forces at all points along L_j are replaced by a single force $\underline{F}_j$ passing through G_j together with a couple with torque $\underline{T}_j$, then $\underline{F}_j$ and $\underline{T}_j$ may be expressed as:

$$\underline{F}_j = \underline{F}_M + \underline{F}_N + \underline{F}_T + \underline{W} + \underline{B}_N \tag{15}$$

and

$$\underline{T}_j = \underline{T}_M + \underline{T}_N \tag{16}$$

where $\underline{F}_M$, $\underline{F}_N$, $\underline{F}_T$, $\underline{W}$, and $\underline{B}_N$ are due to the added mass, normal drag, tangential drag, gravity and buoyancy forces respectively, and $\underline{T}_M$ and $\underline{T}_N$ are torques due to the added mass and normal drag forces. These forces and torques may be expressed as [2]:

$$F_M = AL\underline{a}_{GN} \tag{17}$$

$$F_N = B\{\underline{\omega}x \, \underline{n}(1/3c)(x^{3/2}\big|_{-L/2} - x^{3/2}\big|_{L/2}) + [(b/2c)\underline{\omega} \times \underline{n}$$
$$+ \underline{v}_{GN}]\left[\left(\frac{cL+b}{4c}\right)x^{1/2}\big|_{L/2} + \left(\frac{cL-b}{4c}\right)x^{1/2}\big|_{-L/2} \right.$$
$$\left. + \left(\frac{4ac-b^2}{8c^{3/2}}\right)\log\left(\frac{x^{1/2}\big|_{L/2} + (Lc^{1/2}/2) + (b/2c^{1/2})}{x^{1/2}\big|_{-L/2} - (Lc^{1/2}/2) + (b/2c^{1/2})}\right)\right]\} \tag{18}$$

-6-

$$\underline{F}_T = CL|\underline{V}_{GT}|\underline{V}_{GT} \tag{19}$$

$$\underline{W} = \underline{w}L = -\rho_c gL\underline{k} \tag{20}$$

$$\underline{B}_N = \underline{b}_N L = \rho gaL\ \underline{n} \times (\underline{k} \times \underline{n}) \tag{21}$$

$$\underline{T}_M = -A(L^3/12)[\underline{\alpha} - (\underline{\alpha} \cdot \underline{n})\underline{n} + (\underline{\omega} \cdot \underline{n})\underline{n} \times \underline{\omega}] \tag{22}$$

and

$$\underline{T}_N = B\underline{n} \times \underline{V}_{GN}\Big[(1/3c)X^{3/2}\Big|_{L/2} - (1/3c)X^{3/2}\Big|_{-L/2} - \frac{b(cL+b)}{8c^2}X^{1/2}\Big|_{L/2}$$

$$+ \frac{b(-cL+b)}{8c^2}X^{1/2}\Big|_{-L/2} - \frac{b(4ac-b^2)}{16c^{5/2}}\log\left(\frac{X^{1/2}\big|_{L/2}+(Lc^{1/2}/2)+(b/2c^{1/2})}{X^{1/2}\big|_{-L/2}-(Lc^{1/2}/2)+(b/2c^{1/2})}\right)$$

$$+ B[(\underline{\omega} \cdot \underline{n})\underline{n} - \underline{\omega}]\{(1/4c)[(L/2) - (5b/6c)]X^{3/2}\Big|_{L/2} \tag{23}$$

$$+ (1/4c)[(L/2) + (5b/6c)]X^{3/2}\Big|_{-L/2}$$

$$+ [5b^2 - 4ac)/16c^2]\left[\frac{cL+b}{4c}X^{1/2}\Big|_{L/2} + \frac{cL-b}{4c}X^{1/2}\Big|_{-L/2}\right.$$

$$\left. + \left(\frac{4ac-b^2}{8c^{3/2}}\right)\log\left(\frac{X^{1/2}\big|_{L/2}+(Lc^{1/2}/2)+(b/2c^{1/2})}{X^{1/2}\big|_{-L/2}-(Lc^{1/2}/2)+(b/2c^{1/2})}\right)\Big]\Big\}$$

where L is the length of L_j, $\underline{\omega}$ and $\underline{\alpha}$ are the angular velocity and angular acceleration of L_j, and $\underline{v}_{GN}$ and $\underline{a}_{GN}$ are the components of the fluid velocity and acceleration normal to L_j at G_j. $\underline{V}_{GN}$ and $\underline{a}_{GN}$ may be expressed as:

$$\underline{V}_{GN} = \underline{V}_{W/G} - (\underline{V}_{W/G} \cdot \underline{n})\underline{n} \tag{24}$$

and

$$\underline{a}_{GN} = \underline{a}_{W/G} - (\underline{a}_{W/G} \cdot \underline{n})\underline{n} \tag{25}$$

where $\underline{V}_{W/G}$ and $\underline{a}_{W/G}$ are the velocity and acceleration of the fluid relative to G_j. Finally, the coefficients a, b, and c, and X are:

$$a = \underline{V}_{GN} \cdot \underline{V}_{GN} \tag{26}$$

$$b = -2\underline{V}_{GN} \cdot \underline{\omega} \times \underline{n} \tag{27}$$

$$c = (\underline{\omega} \times \underline{r}) \cdot (\underline{\omega} \times \underline{n}) \tag{28}$$

and

$$X = a + bx + cx^2 \tag{29}$$

where x is the length variable shown in Figure 2.

Using these results, the generalized active forces F_ℓ are:

$$F_\ell = v_{j\ell k}F_{jk} + \omega_{j\ell k}T_{jk} \tag{30}$$

where F_{jk} and T_{jk} are the n_k components of $\underline{F}_j$ and $\underline{T}_j$ of Equations (15) and (16). (As before, there is a sum in Equation (30) over the repeated indices for the range of the indices.)

III. SUBMERGED CABLE DYNAMICS

Analytical validation of the finite segment model (UCIN-CABLE) without fluid forces, has been obtained by comparing results predicted by the model with results obtained using other methods. Reference [3] records details of this validation. To obtain additional validation, and to develop further applications, a series of _submerged_ cable maneuvers were simulated. These included buoy relaxations and achor drops in water depicted in Figure 3.

In each maneuver, the cable length was 72 in. (1.83 m). Silicon rubber and nylon cables were simulated. The silicon rubber cable had a diameter of 0.163 in. (4.14 mm) and the nylon cable had a diameter of 0.1 in. (2.54 mm). The weight densities of the silicon rubber cables were 0.137 lb/in (24.0 N/m) and 0.108 lb/in (18.92 N/m) in air. (The heavier cable included a wire conductor.) The weight density of the nylon cable was 0.0448 lb/in (7.85 N/m) in air. The buoys and anchors were 2 in. (50.8 mm) diameter spheres weighing 0.025 lb (0.111 N) and 0.246 lb (1.09 N) in air respectively.

a. Bouy Relaxation b. Anchor Drop
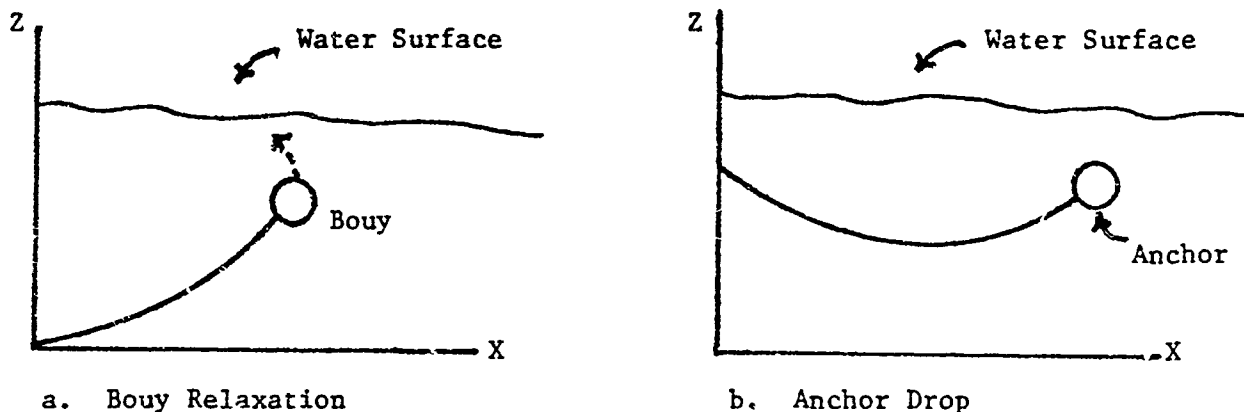
Figure 3. Cable Maneuvers.

Six tests were conducted. The first four were buoy relaxations as
in Figure 3a. The last two were anchor drops as in Figure 3b. Twelve
identical cable segments together with a sphere representing the buoy
or anchor, were used in the model, for each test. The fluid mass density
and viscoscity were given the values 1.9856 slug/ft^3 (1024.16 kg/m^3) and
3.516 x 10^{-5} slug/ft.sec. (1.684 x 10^{-3} kg/m sec) to simulate seawater.

The tests were designed to simulate experimental tests conducted at
the Civil Engineering Laboratory in Port Hueneme, CA as recorded by
Palo [6]. Table I provides a description of the tests. Figures 4. to
9. show the cable configuration at various times, together with compar-
isons with experimental results and finite element results (SEADYN) for
the respective tests. Figures 10. to 15. show analogous results for
the fixed end tension. Finally, Figures 16. to 21. show buoy and anchor velocities.

Test Number	Type	Initial Position of Buoy or Anchor (See Figure 3.)	Cable Material
1	Buoy Relaxation	x = 51 in., z = -24 in.	Silicon Rubber
2	Buoy Relaxation	x = 51 in., z = -33 in.	Silicon Rubber with Wire Core
3	Buoy Relaxation	x = 51 in., z = -33 in.	Nylon
4	Buoy Relaxation	x = 51 in., z = 16.6 in.	Silicon Rubber with Wire Core
5	Anchor Drop	x = 66 in., z = 0	Silicon Rubber
6	Anchor Drop	x = 54 in., z = 0	Silicon Rubber

Table I. Test Descriptions.
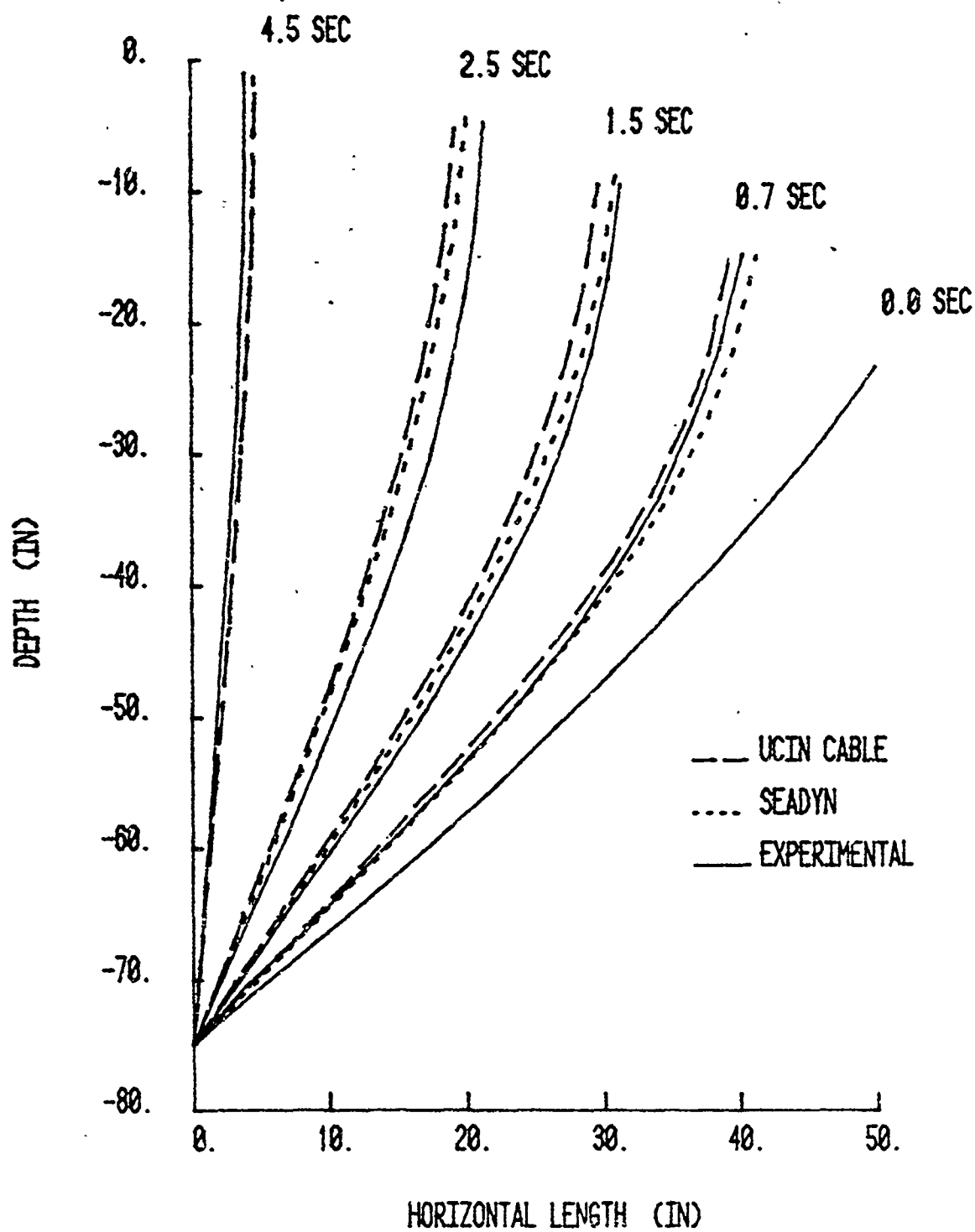
Figure 4. Test 1: Configurations for Buoy Relaxation
For Rubber Cable.
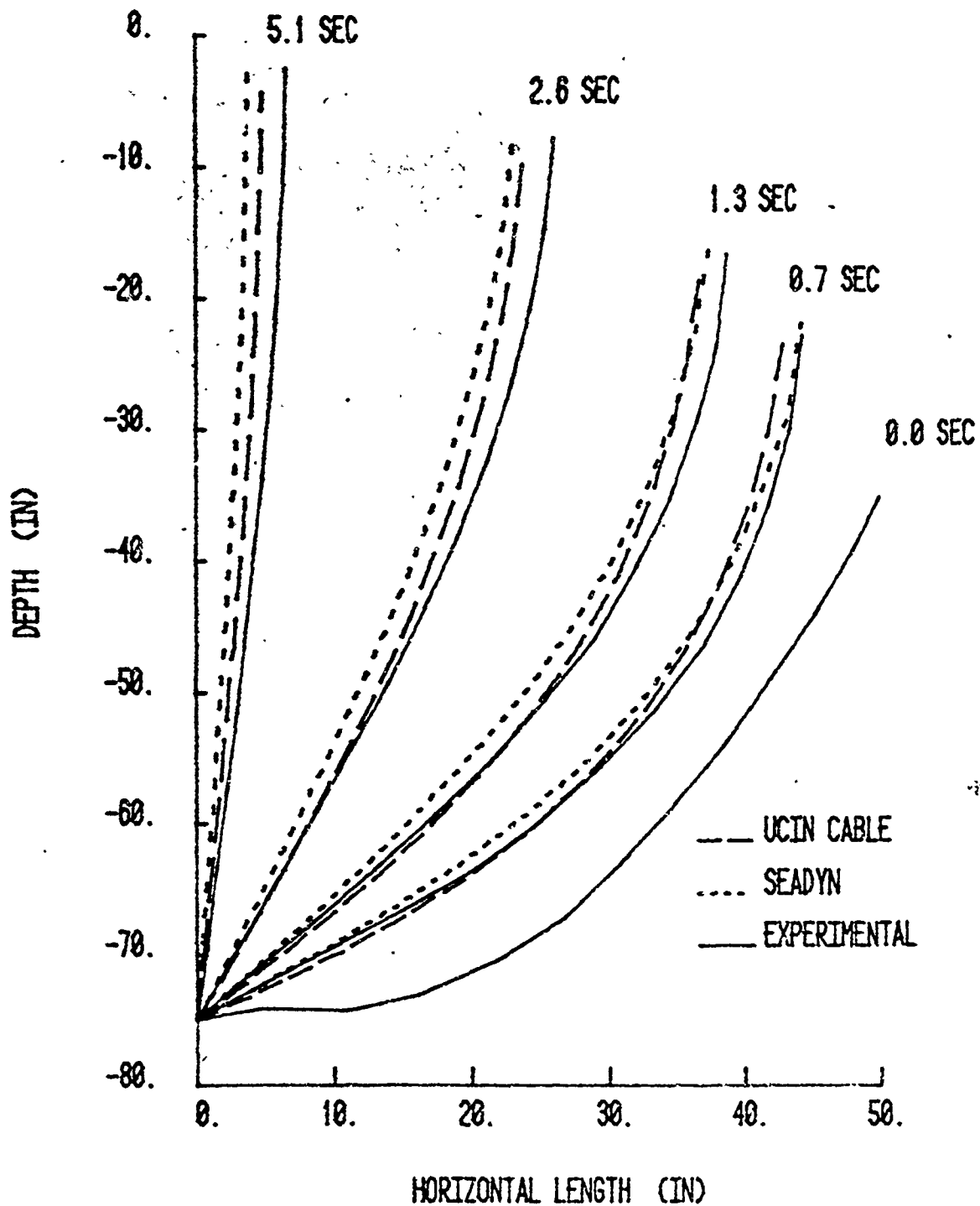
Figure 5. Test 2: Configurations for Buoy Relaxation
for Rubber Cable with Wire Core.
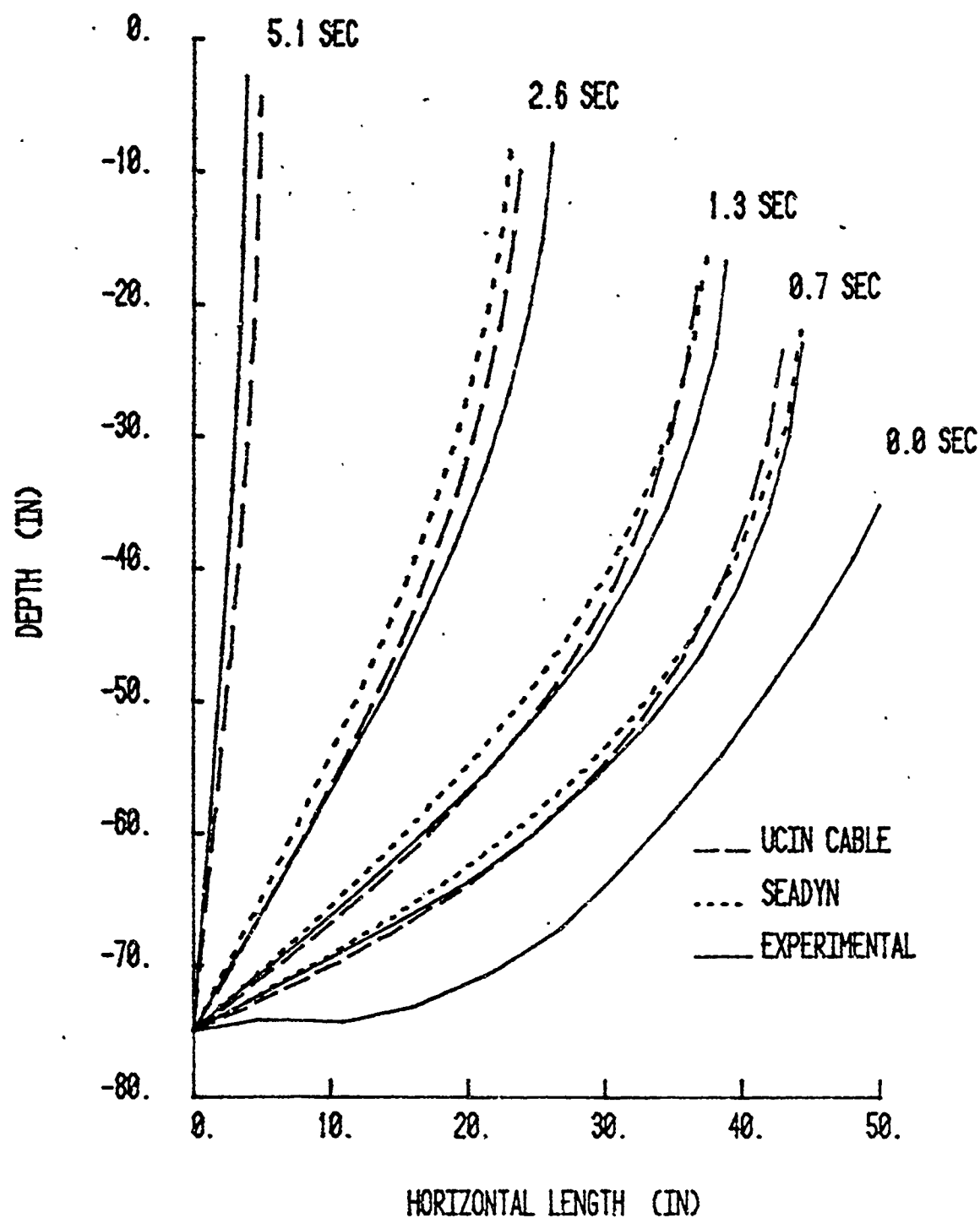
Figure 6.   Test 3:   Configurations for Buoy Relaxation
for Nylon Cable.
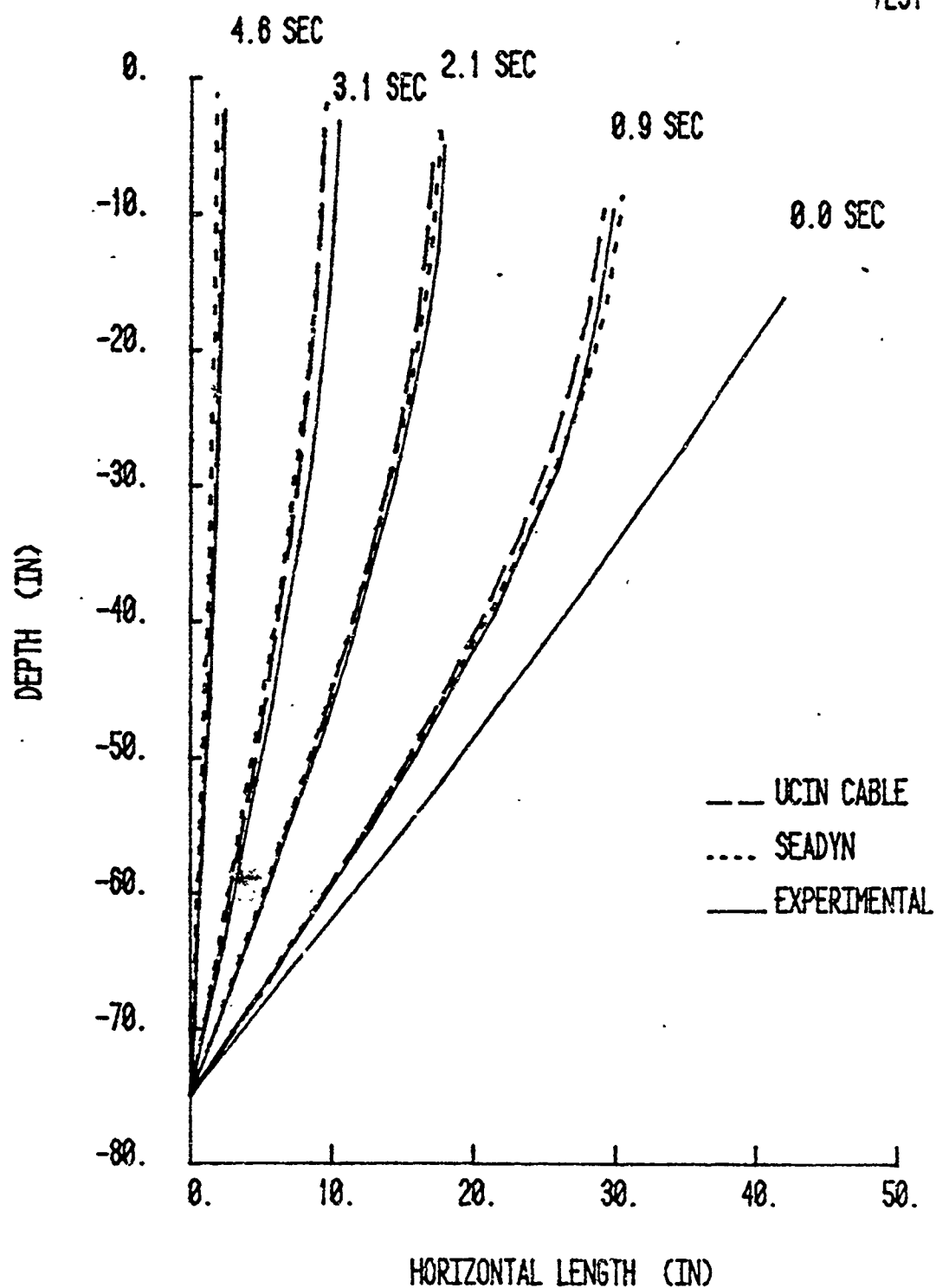
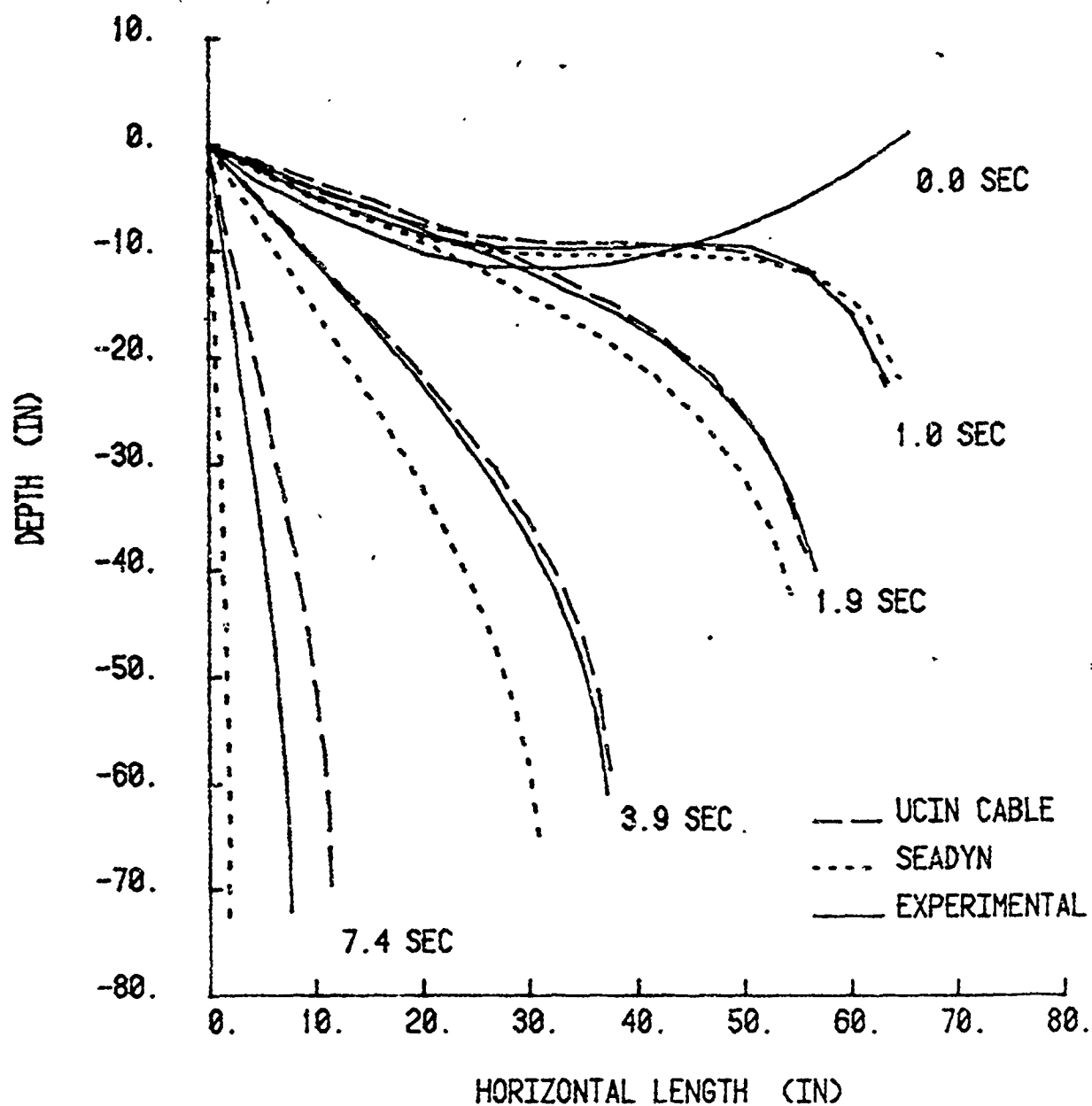Figure 7. Test 4: Configurations for Buoy Relaxations
for Rubber Cable with Wire Core.

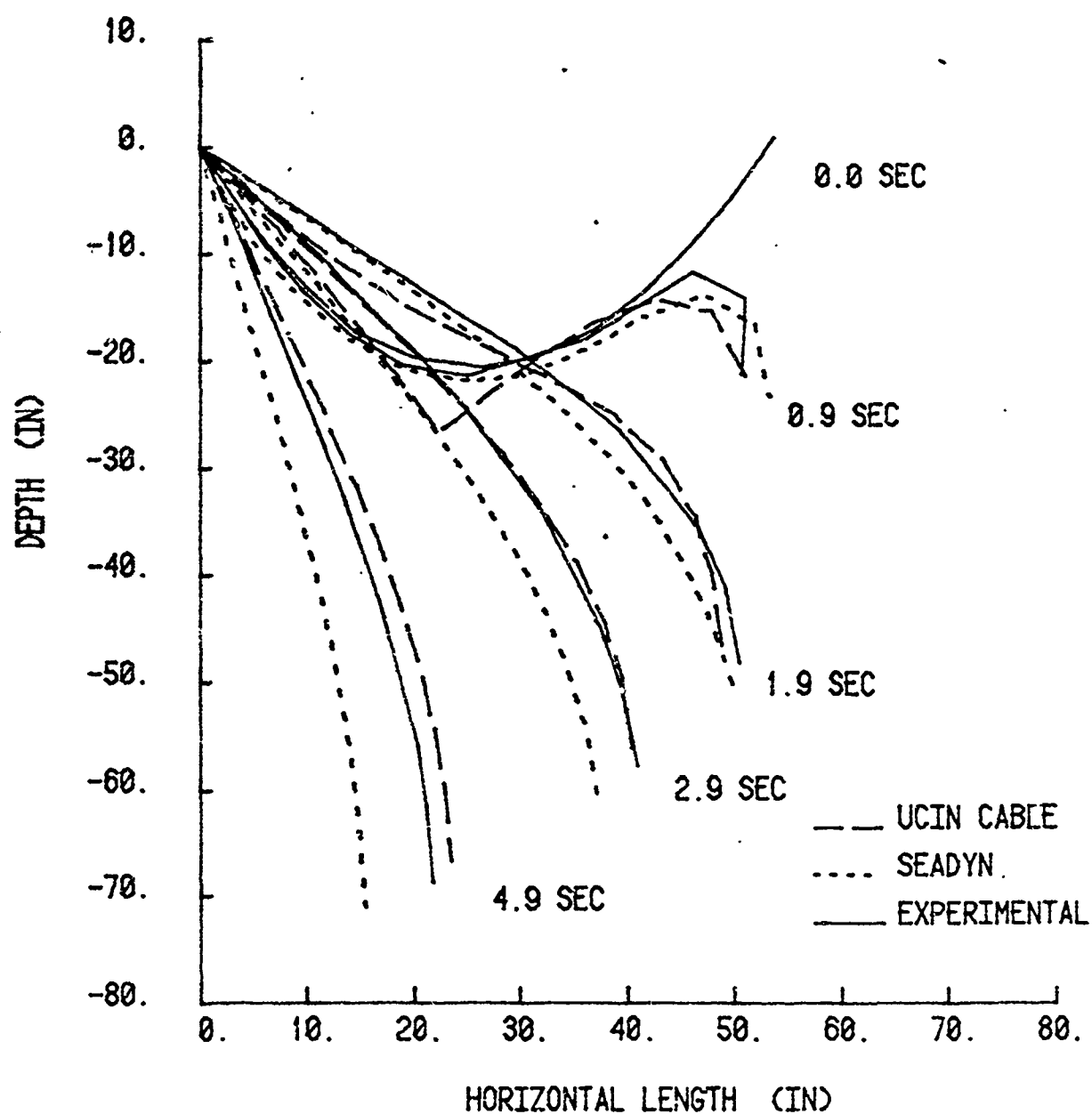Figure 8. Test 5: Configurations for Anchor Drop for Rubber Cable.

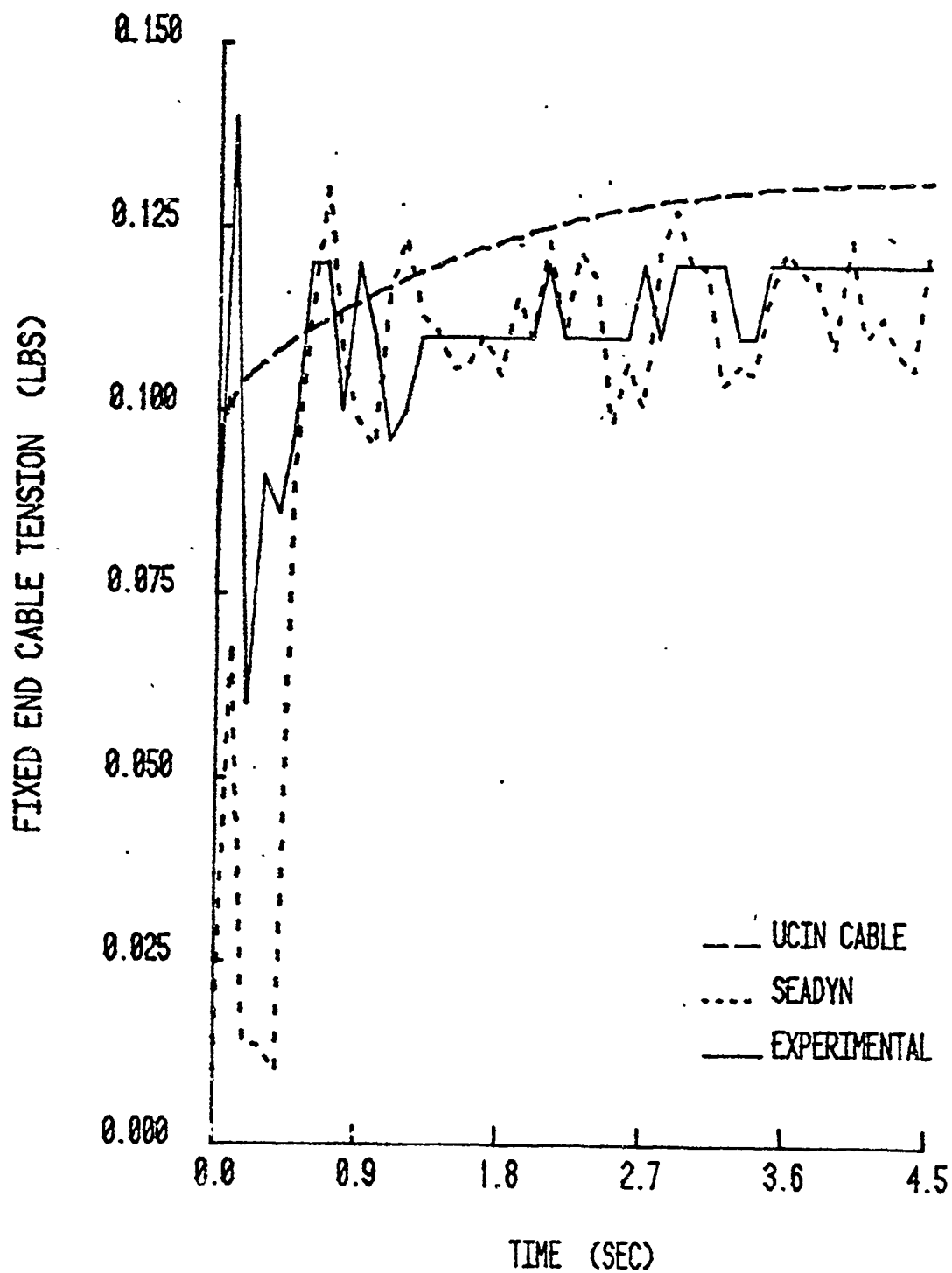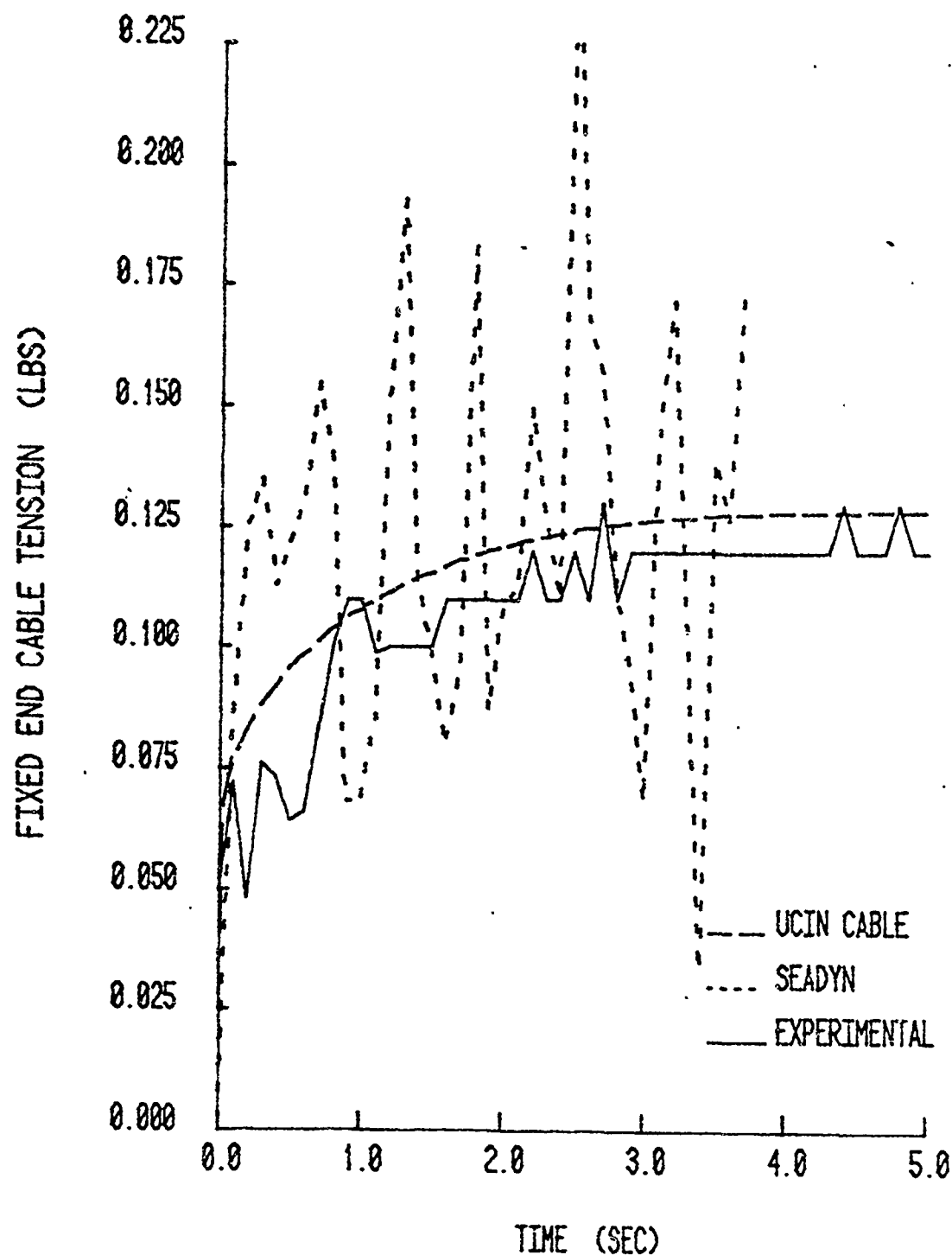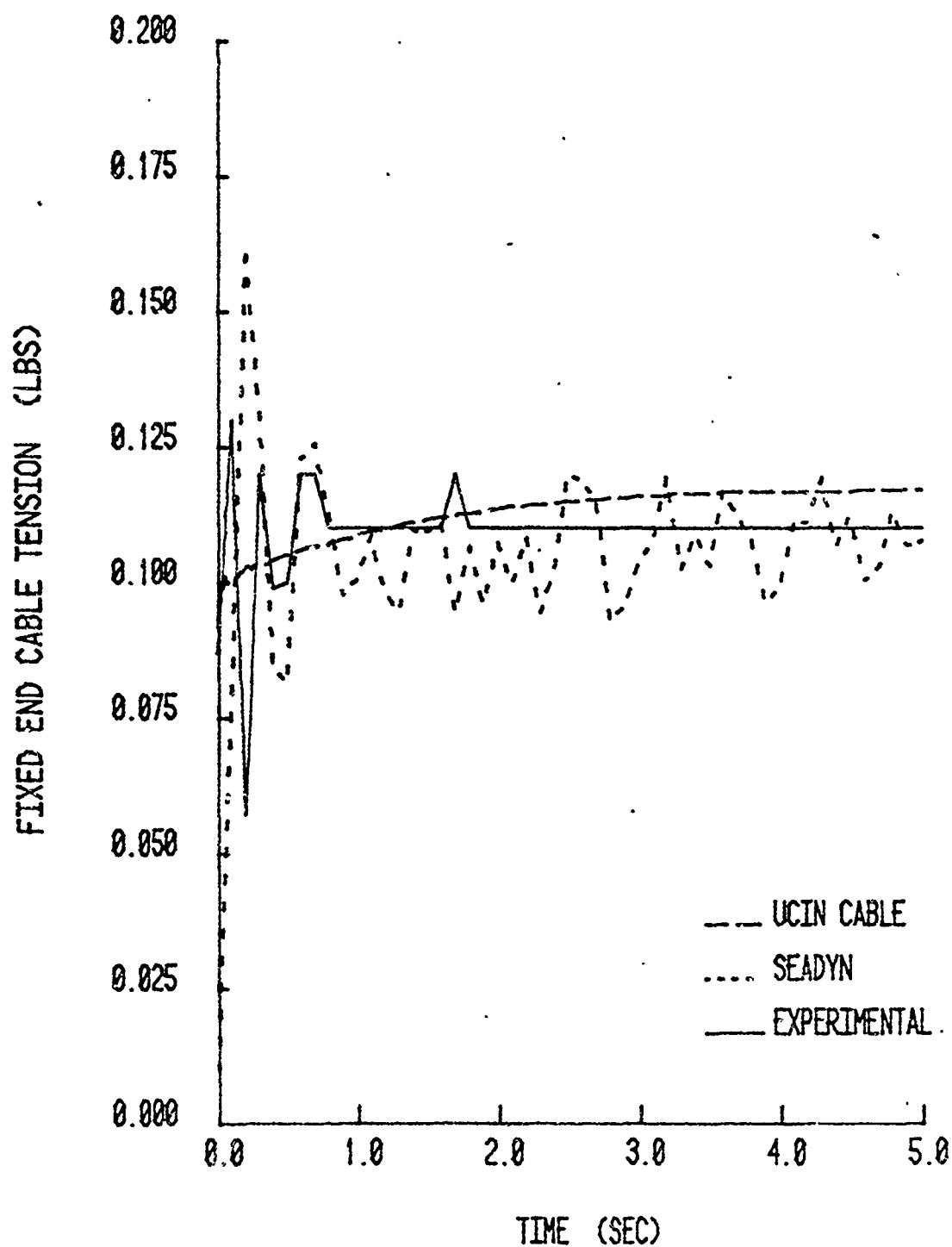Figure 9. Test 6: Configurations for Anchor Drop for Rubber Cable.

Figure 10. Test 1: Fixed End Tension for Buoy Relaxation for Rubber Cable.
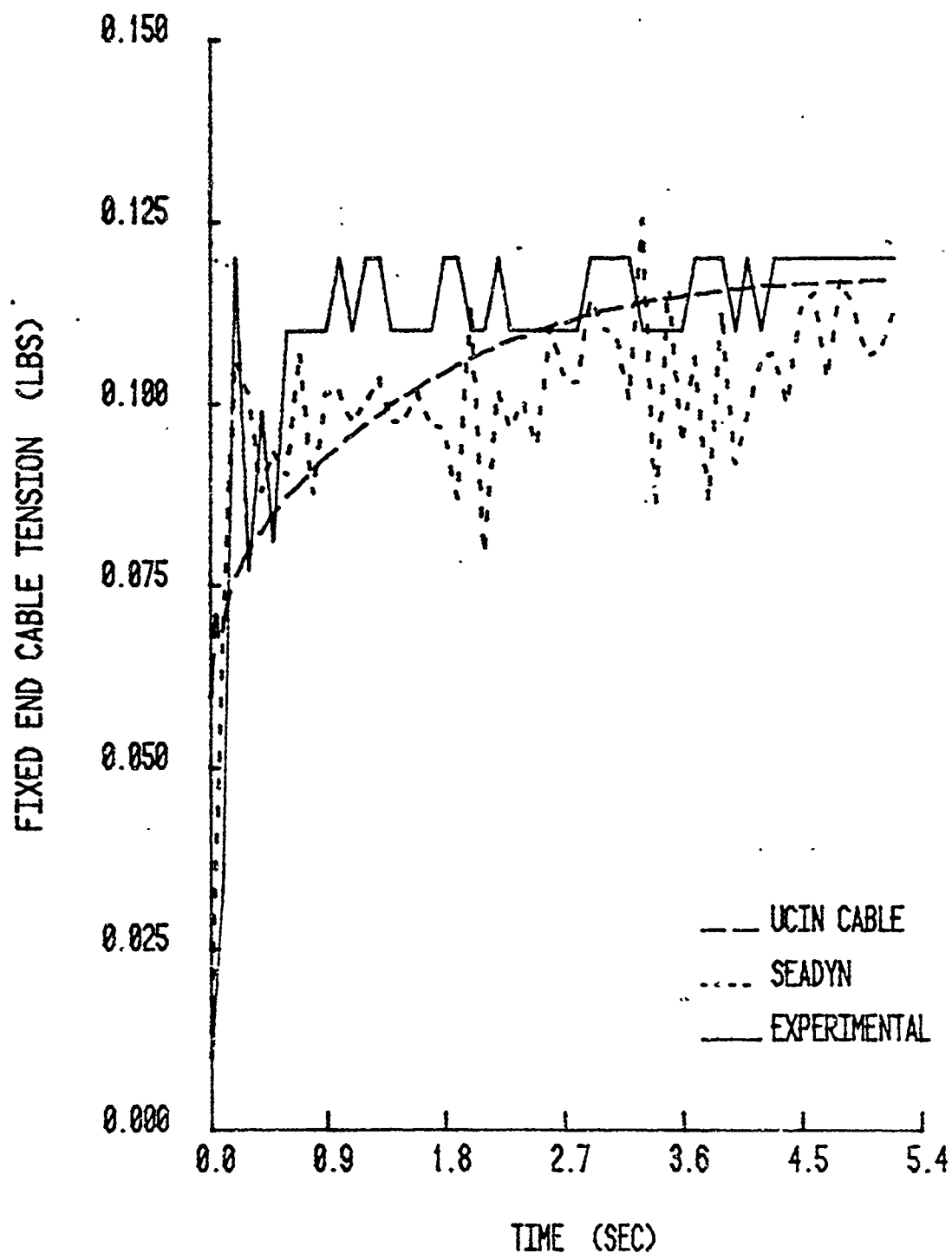
Figure 11. Test 2: Fixed End Tension for Buoy Relaxation for Rubber Cable with Wire Core.

Figure 12.   Test 3:   Fixed End Tension for Buoy Relaxation
for Nylon Cable.

Figure 13. Test 4: Fixed End Tension for Buoy Relaxation for Rubber Cable with Wire Core.
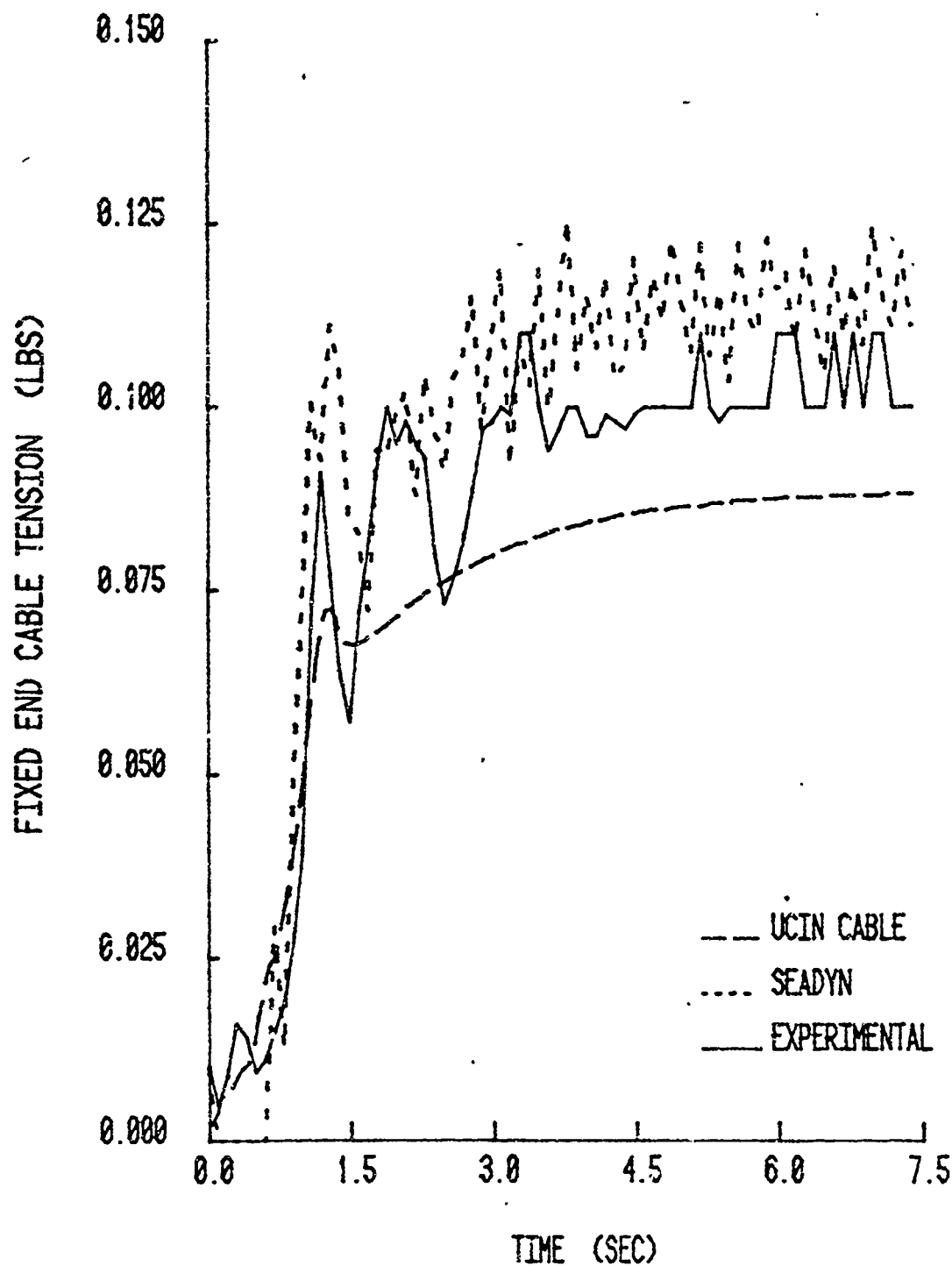
Figure 14. Test 5: Fixed End Tension for Anchor Drop for Rubber Cable.
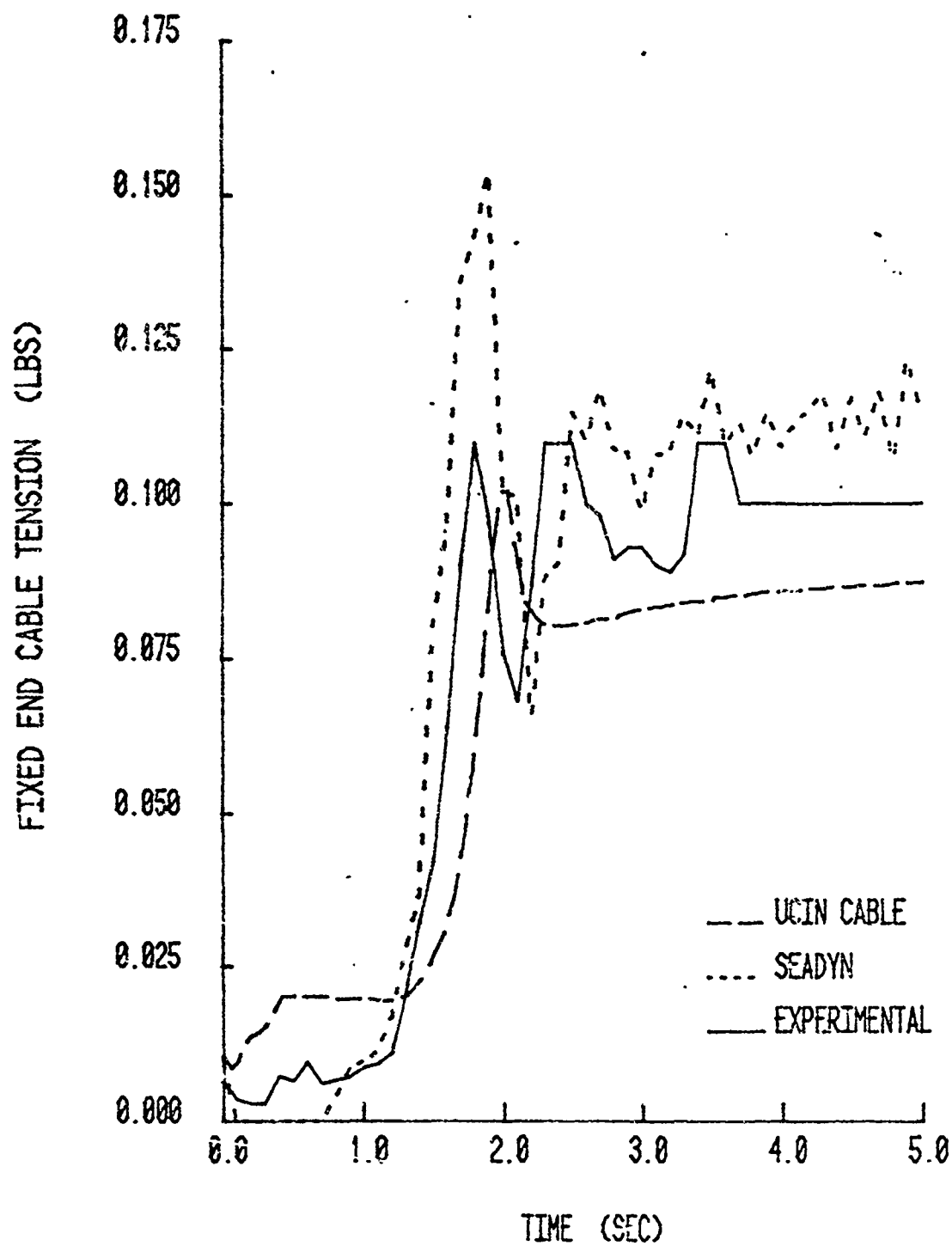
Figure 15.   Test 6:   Fixed End Tension for Anchor Drop for
Rubber Cable.
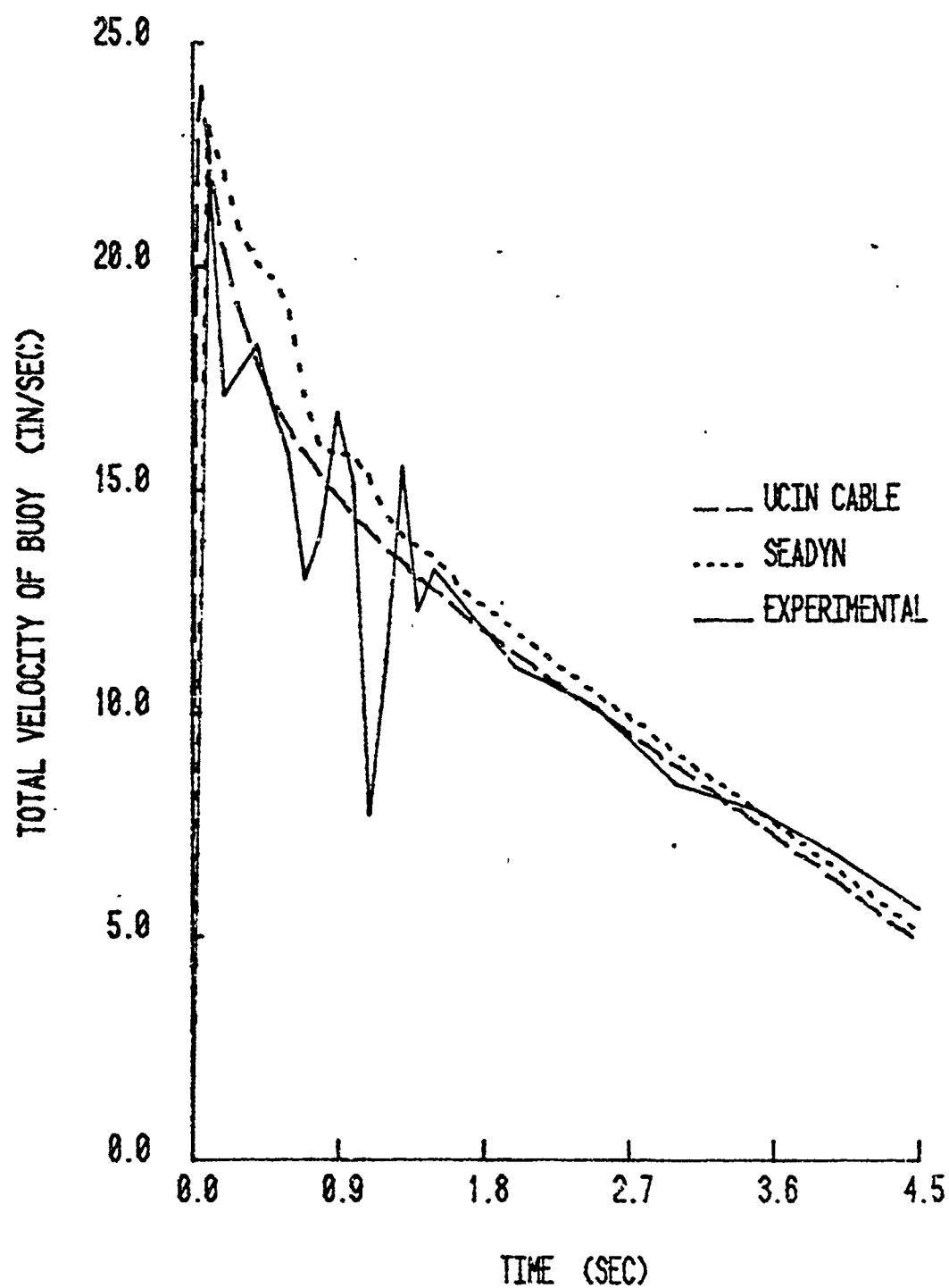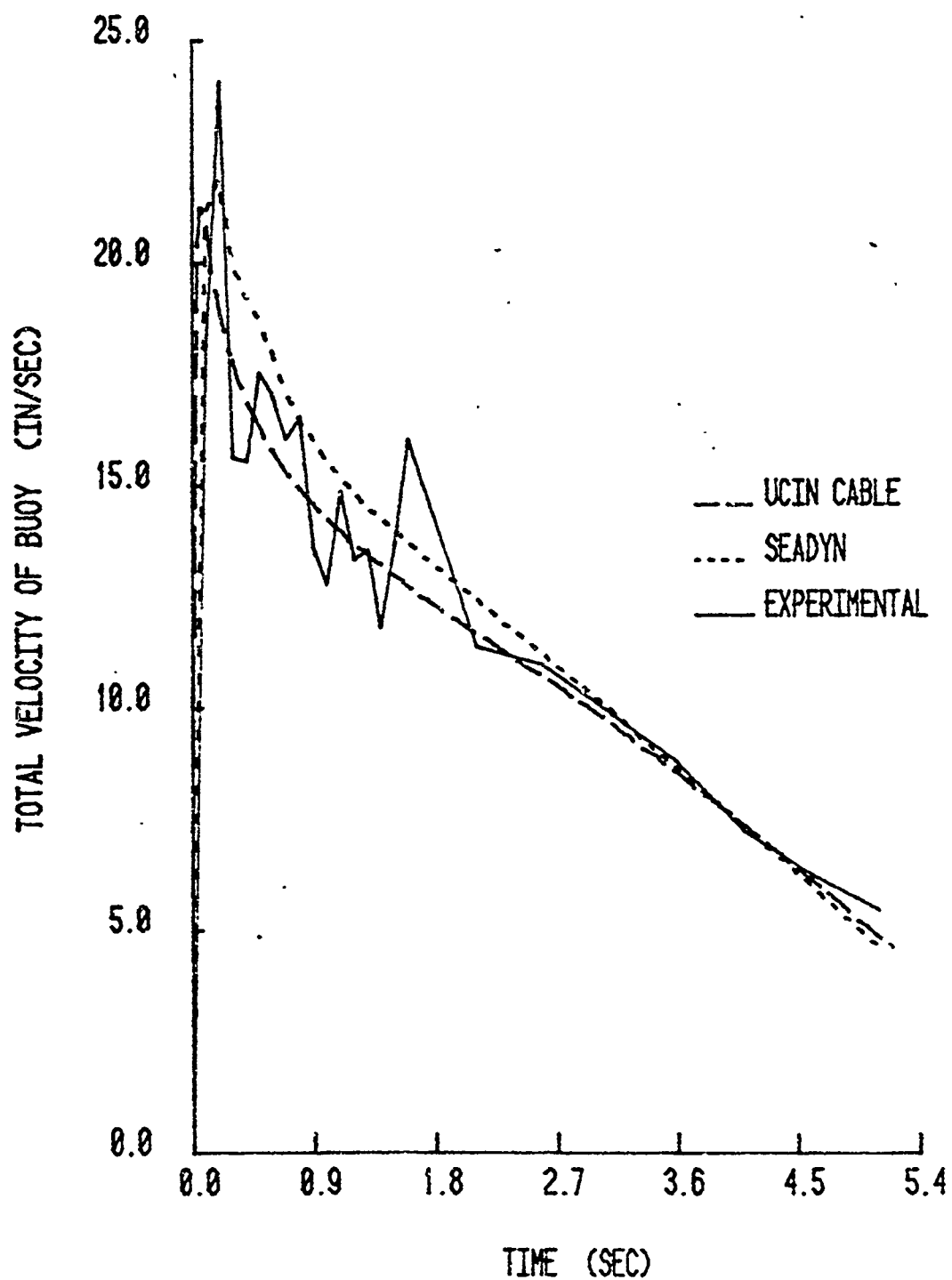
Figure 16. Test 1: Buoy Velocity for Rubber Cable.

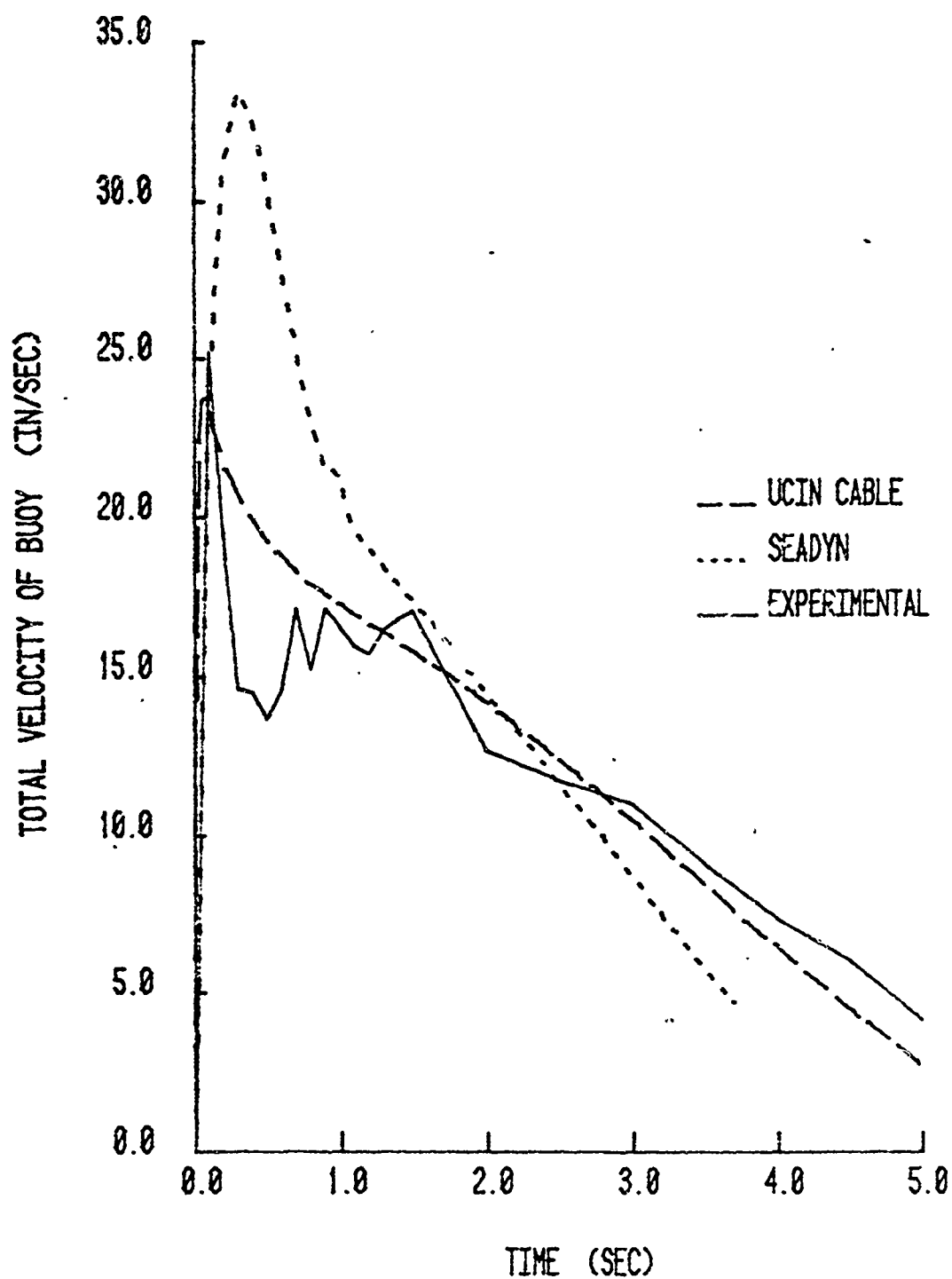Figure 17.   Test 2:   Buoy Velocity for Rubber Cable
with Wire Core.

Figure 18.   Test 3:   Buoy Velocity for Nylon Cable.
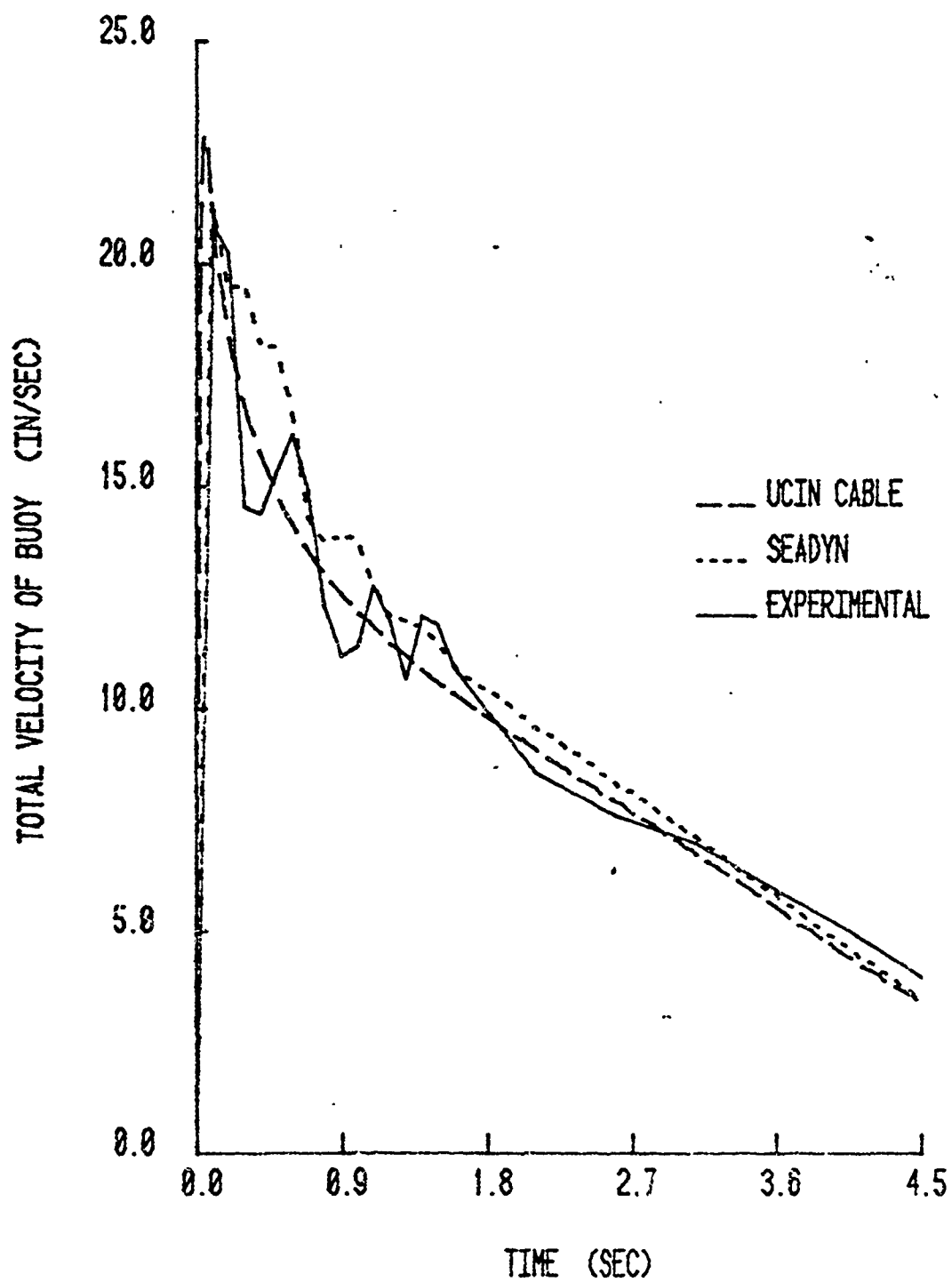
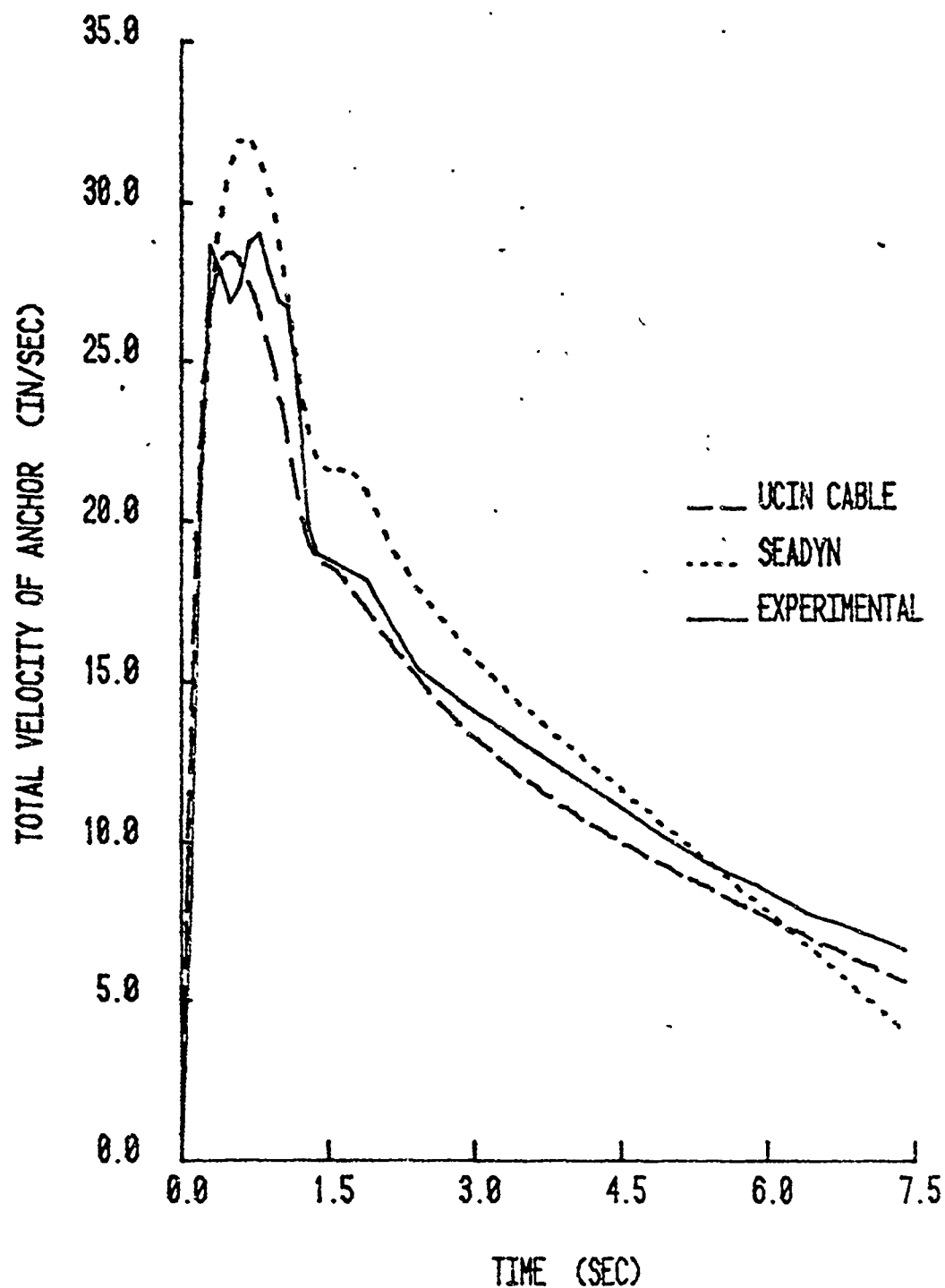Figure 19. Test 4: Buoy Velocity for Rubber Cable with Wire Core.

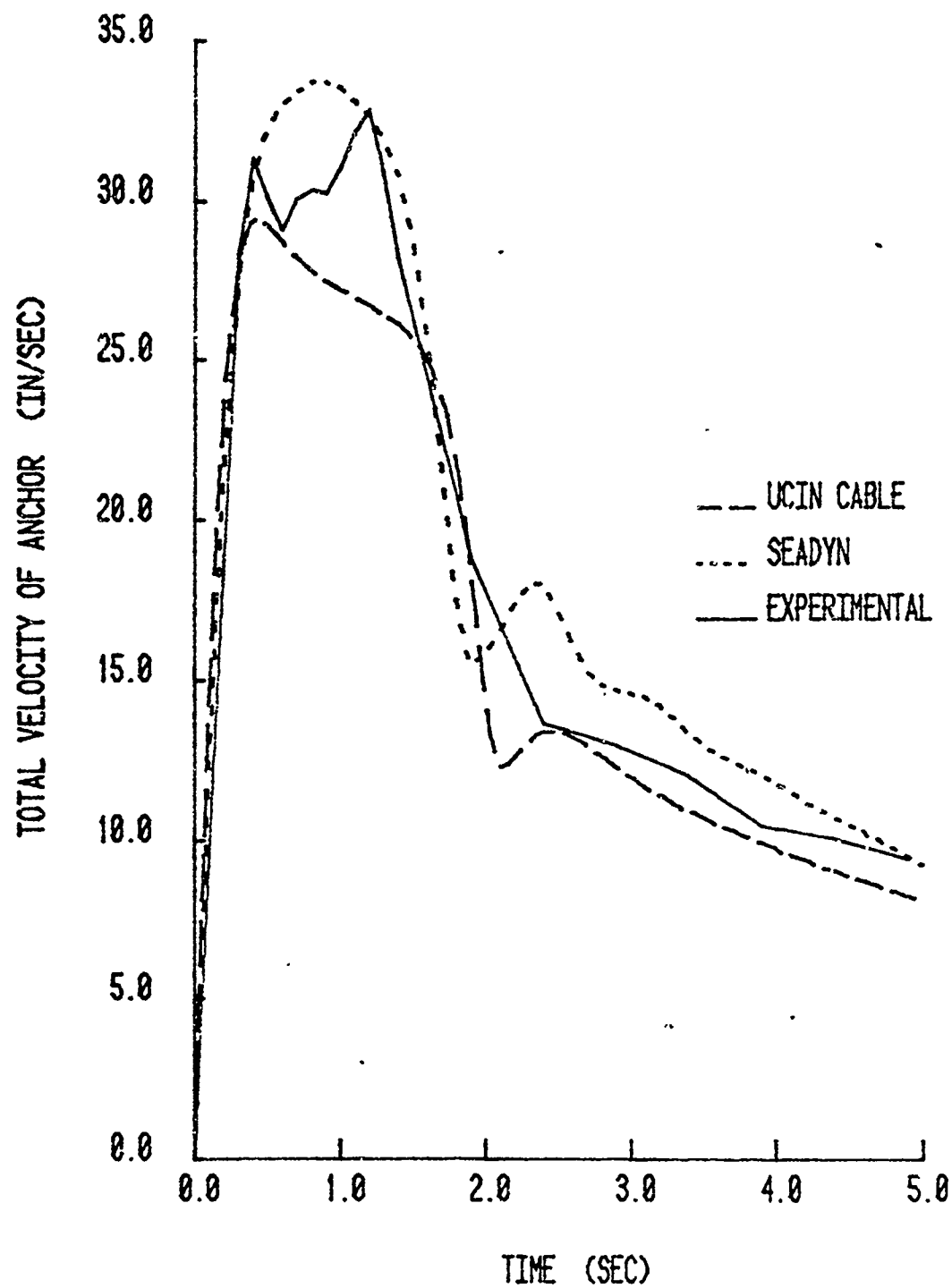Figure 20.   Test 5:   Anchor Velocity for Rubber Cable.

Figure 21.   Test 6:   Anchor Velocity for Rubber Cable.

IV. DISCUSSION AND CONCLUSIONS

In the current set of tests the cable was relatively light.
Hence, the viscous forces were relatively large compared with the
gravitational and inertia forces. The tests thus provide a validation
of the fluid force modelling of the UCIN-CABLE code. (As noted earlier,
the inertia force validation is reported in Reference [3].)

The results show that it is not only possible, but it is also
practical to obtain numerical simulation of cable dynamics through
finite segment modelling. What remains is a validation of the
modelling for three-dimensional maneuvers.

ACKNOWLEDGEMENT

REFERENCES

1. Winget, J. M., and Huston, R. L.,"Cable Dynamics - A Finite Segment Approach," Computers and Structures, Vol. 6, 1976, pp. 475-480.

2. Huston, R. L., and Kamman, J. W., "A Representation of Fluid Forces in Finite Segment Cable Models," Computers and Structures, Vol. 14, 1981, pp. 281-287.

3. Huston, R. L., and Kamman, J. W., "Validation of Finite Segment Cable Models," Computers and Structures (in press).

4. Huston, R. L., Passerello, C. E., and Harlow, M. W., "Dynamics of Multi-Rigid-Body Systems," Journal of Applied Mechanics, Vol. 45, 1978, pp. 889-894.

5. Huston, R. L., and Passerello, C. E., "On Multi-Rigid-Body Systems Dynamics," Computers and Structures, Vol. 10, 1979, pp. 439-446.

6. Palo, P. A., "Comparisons Between Small-Scale Cable Dynamics Experimental Results and Simulations Using SEADYN and SNAPLG Computer Models," Technical Memorandum TM No. M-44-79-5, Civil Engineering Laboratory, Port Hueneme, CA, 1979.

7. Webster, R. L., "An Application of the Finite Element Method to the Determination of Nonlinear Static and Dynamic Responses of Underwater Cable Structures," General Electric Technical Information Series Report No. R76EMH2, Syracuse, NY, 1976.

8. Kane, T. R., P. W. Likins, and D. A. Levinson, Spacecraft Dynamics, McGraw Hill, 1983.

9. Brand, L., Vector and Tensor Analysis, Wiley, New York, 1947.